An Analytical Position Correction Algorithm for γ-Camera Planar Images from Resistive Chain Readouts

D. Thanasas, E. Georgiou, N. Giokaris, A. Karabarbounis, D. Maintas, M. Mikeli, C.N. Papanicolas, L. Ragkousis and E. Stiliaris, *Member, IEEE*

***Abstract*–The charge limitation for peripheral Field Of View (FOV) events detected by the most commonly used Position Sensitive Photomultiplier Tubes (PSPMTs) results to spatial distortions and non-uniformities of the obtained planar images. These effects can be corrected with newly developed sophisticated techniques operating on the charge signals from the individual wires of the multi-anode systems. However, a similar algorithmic approach for the simple case, where the resistive chain readout technique is used and, consequently, the original charge distribution information is lost, is not applicable. In this work the development of a new method to eliminate these distortion effects in the planar images for γ-Camera systems based on resistive chain techniques is presented. The proposed model, which incorporates an a priori knowledge of three parameters related to light diffusion inside the scintillation crystal in use, provides an accurate, analytically calculated estimate of the spatial correction as a function of the primary reconstructed planar position from the resistive chain signals. This algorithm can be used online on an event-by-event basis and can be applied to both, homogeneous and pixelated crystals.**

I. Introduction

In nuclear medicine, many small field, high-resolution γ-Camera systems based on PSPMTs, have been recently developed [1-3]. Their advantages over commercial γ-Camera systems (better spatial resolution, lower cost, light weight) justify their demand for imaging either small human body organs or small animals. PSPMTs are technologically advanced photomultiplier tubes with a multi-wire anodic grid instead of a simple anode. Using PSPMTs, information about both the energy and the position of an event, can be extracted using the appropriate reconstruction techniques.

Readout techniques mostly used with PSPMTs can be separated into two categories: The Individual Signal Readout (ISR) technique, where the charge of each wire (X_1, X_2,…, X_N and Y_1, Y_2,…, Y_N) is separately recorded and the Resistive Chain Readout (RCR) technique, which leads to only two signals for each axis (X_A, X_B, Y_C and Y_D) after the application of the appropriate resistor-chain (Fig.1). Although the ISR technique provides information about the charge distribution on the anodic grid, the RCR loses this information.

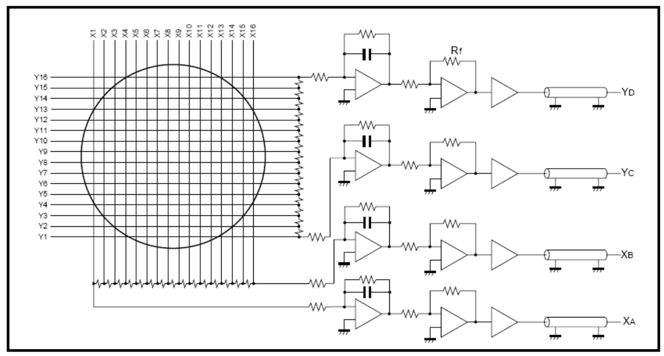

Fig.1. The multi-wire anodic grid of the R2486 HAMAMATSU PSPMT with the Resistive Chain Readout (RCR) technique. Individual readout of each wire is also possible (Individual Signal Readout - ISR).

In both cases, the energy and the position of an incident photon can be reconstructed through the equations (1) and (2) or (3) and (4) for the ISR and RCR respectively. In Equation (2) the position is reconstructed, using the Center Of Gravity (COG) algorithm applied on the charge distribution. Due to the linearity of the reconstruction, it can be proved that the Resistive Chain (RC) and COG algorithms are equivalent.

$$E_{COG} = \sum_{i=1}^{N} (Qx_i + Qy_i) \quad (1)$$

$$X_{COG} = \frac{\sum_{i=1}^{N} i \cdot Qx_i}{\sum_{i=1}^{N} Qx_i}, \quad Y_{COG} = \frac{\sum_{i=1}^{N} i \cdot Qy_i}{\sum_{i=1}^{N} Qy_i} \quad (2)$$

$$E_{RC} = X_A + X_B + Y_C + Y_D \quad (3)$$

$$X_{RC} = \frac{X_A - X_B}{X_A + X_B}, \quad Y_{RC} = \frac{Y_C - Y_D}{Y_C + Y_D} \quad (4)$$

Unfortunately, both position reconstruction methods lead to systematic errors. The charge limitations mainly of non-

The work is partially supported by the PENED (03 EΔ 287) research project, implemented within the framework of the “Reinforcement Programme of Human Research Manpower” (PENED) and co-financed by National and Community Funds (25% from the Greek Ministry of Development-General Secretariat of Research and Technology and 75% from E.U.-European Social Fund). The financial support by the program KAPODISTRIAS (Special Account for Research Grants) of the National and Kapodistrian University of Athens is gratefully acknowledged.

D. Thanasas, N. Giokaris, A. Karabarbounis, M. Mikeli, C.N. Papanicolas, L. Ragkousis and E. Stiliaris are with National and Kapodistrian University of Athens, Department of Physics, 15771 Athens, Greece.

E. Georgiou is with National and Kapodistrian University of Athens, Medical School, Athens, Greece.

D. Maintas is with the Institute of Isotopic Studies, Athens, Greece.

Corresponding Author: E. Stiliaris (email: stiliaris@phys.uoa.gr)

9781-4244-3962-1/09/$25.00 ©2009 IEEE

central events produce non-linearities in the information of the position, which are greater at the outer regions of the FOV, as shown in Fig.2.

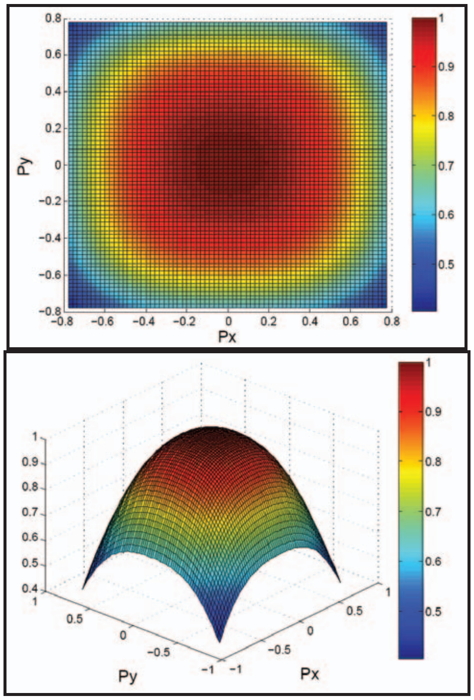

Fig.2. Normalized charge density distribution on the planar area of a PSPMT. Charge limitation reaches a maximum at the periphery of the FOV.

In praxis, the reconstructed position of an incident photon coincides with its nominal value when it falls in the central area. However, this is an ideal case (Fig.3a). Most of the times, the position of a γ-incident photon is systematically different from its nominal value, due to the charge limitations discussed previously (Fig.3b).

These deviations led to the development of a new procedure.

Having constructed a model, according to which one is able to calculate the charge Q_i of the i[th] PSPMT-wire as a function of the photon incident coordinates (Px, Py), it is possible to invert the whole methodology and to determine the incident position from the measured charge distribution. This inversion can be potentially applied to measured data in order to correctly reconstruct the position and to overcome the non-linearities due to discussed limitations.

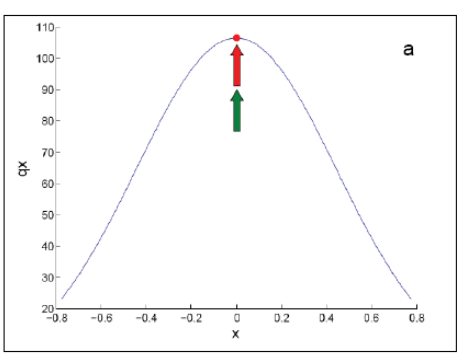

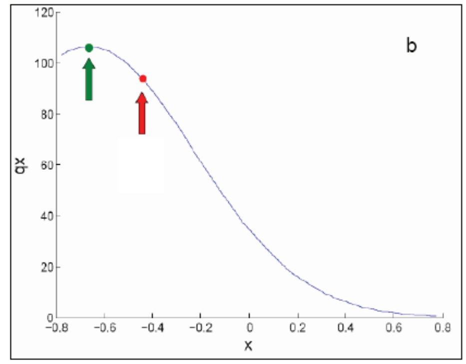

Fig.3. a) Ideal case event, where the reconstructed position (red arrow) of an incident photon coincides with its nominal position (green arrow). b) In the most common cases, the reconstructed position (red arrow) differs from its nominal value (green arrow).

II. MODEL DESCRIPTION

The proposed model for ISR technique as described in [4], parameterizes the incident light with the sum of two Gaussian distributions G_1 and G_2 given by the Equations (5). The charge of the i[th] wire is calculated through the charge density integration along the specific wire using Equations (6). As shown in the formalism, each Gaussian distribution includes two free parameters, the amplitude A and width s.

$$
\begin{aligned}
&G(P_x,P_y,x,y)=G_1(P_x,P_y,x,y)+G_2(P_x,P_y,x,y)\\
&G_1(P_x,P_y,x,y)=A_1\cdot e^{-\frac{(x-P_x)^2+(y-P_y)^2}{2s_1^2}}\\
&G_2(P_x,P_y,x,y)=A_2\cdot e^{-\frac{(x-P_x)^2+(y-P_y)^2}{2s_2^2}}
\end{aligned}
\tag{5}
$$

$$
\begin{aligned}
&X_{Wire}: \quad Qx_i(P_x,P_y,x_i)=k\int_{y_1}^{y_2} G(P_x,P_y,x_i,y)\,dy\\
&Y_{Wire}: \quad Qy_i(P_x,P_y,y_i)=k\int_{x_1}^{x_2} G(P_x,P_y,x,y_i)\,dx
\end{aligned}
\tag{6}
$$

Since the charge values (Qx_i, Qy_i) are recorded with the ISR technique during the experimental procedure, the nominal coordinates (P_x, P_y) of an incident photon can be calculated inverting the proposed model. In order to fix the free parameters of the distributions, the chi-square value of the difference between experimental and calculated charges is minimized. Thus, the optimal coordinates (P_x, P_y) of every incident photon are simultaneously extracted.

Unfortunately, a similar approach can not be applied for the calculation of (P_x, P_y) in the case of the RCR technique. Therefore, the previous model is extended to calculate the signals X_A, X_B and Y_C, Y_D from the Qx_i and Qy_i. This can be easily done by using the following linear equations:

$$X_A = \sum_{i=1}^{N} Qx_i \cdot \frac{N-i}{N}, \quad X_B = \sum_{i=1}^{N} Qx_i \cdot \frac{i}{N} \quad (7)$$

$$Y_C = \sum_{i=1}^{N} Qy_i \cdot \frac{N-i}{N}, \quad Y_D = \sum_{i=1}^{N} Qy_i \cdot \frac{i}{N} \quad (8)$$

By inverting now this procedure the coordinates (P_x, P_y) can be calculated from the four recorded signals (X_A, X_B, Y_C and Y_D). This inversion method, applicable in the case of RCR technique, will be described and discussed in the following section.

III. INVERSE METHOD

In order to apply the extended model to experimental data obtained from a PSPMT with a RCR technique, the free parameters (A_1, s_1) and (A_2, s_2) should have been determined. These free parameters, which characterize the system Scintillation Crystal-PSPMT, can be easily obtained with an experimental procedure based on the ISR technique. These values are unique for each crystal and depend only on its material and its thickness for specific energy of the emitted photons.

This characterization can be done using the minimization process described in section II. It must be noted that in case of a pixelated scintillation crystal all the parameters s_1, s_2 and the ratio A_1/A_2 must be defined, but in case of a homogeneous crystal only one Gaussian distribution is necessary to successfully describe the light output of the crystal.

After its characterization (for various photon energies), a crystal can then be used as the detector of a system using the RCR technique. The four output signals and the corresponding reconstructed coordinates (X_{RC}, Y_{RC}) can be tabulated using the described model and equations (7), (8) and (4). As a result, the dependence of X_{RC} (or of Y_{RC}) on the nominal position P_x (or on P_y) can be studied for different values of the parameters s_1, s_2 and A_1/A_2. Curves X_{RC}=f(P_x) and Y_{RC}=f(P_y) can constructed and they can be used as lookup functions for the online (or offline) event reconstruction.

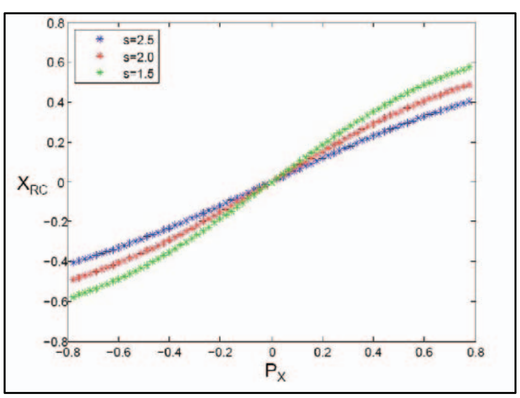

Fig.4. Dependence of the measured position X_{RC} on the nominal position P_x for three different values of the model parameter s in case of a homogeneous crystal.

In Fig.4, the dependence of the measured position X_{RC} on its nominal value P_x is depicted for three different values of the model parameter s in case of a homogeneous crystal. It is obvious that the parameter A does not affect the position reconstruction. As shown in Fig.4, by increasing the parameter s the reconstructed FOV is shrinking and the deviation of the linearity (ideal case) becomes greater.

IV. RESULTS

A. *Reconstruction with pixelated crystal*

The inverse method was applied to data obtained after irradiation (in a RCR system) of a 4mm thick, pixelated CsI(Tl) crystal with a ^{60}Co point source, without using any collimator. The position was reconstructed using the resistive chain algorithm and the inverse method. The pixelated crystal has been characterized, with the help of an ISR system; the values of the parameters needed in the extended model are fixed with $<s_1>=0.7$, $<s_2>=2.1$ and $<A_1/A_2>=10$. The detected planar images are shown in Fig.5.

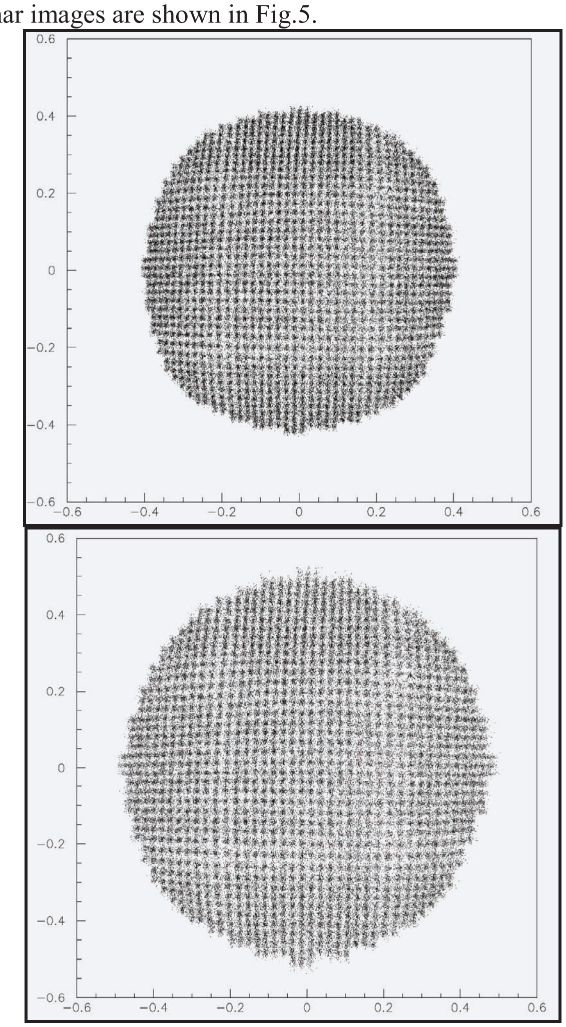

Fig.5. Planar images of a 4mm thick pixelated CsI(Tl) crystal after irradiation with a ^{60}Co point source. Distances are measured in system's units [-1, +1]. Upper Part: The position was reconstructed with the resistive chain algorithm. Lower Part: The position was reconstructed with the inverse method described in this work using for the extended model the parameter values $<s_1>=0.7$, $<s_2>=2.1$ and $<A_1/A_2>=10$.

Comparing the quality of the two planar images, it is obvious that the position reconstruction with the inverse method is better than that with the resistive chain algorithm. The quality of the later image can be further improved by applying the lookup table correction method described in [5]. The final result after both corrections is shown in Fig.6. In the final frame the position is given in true distance values (mm).

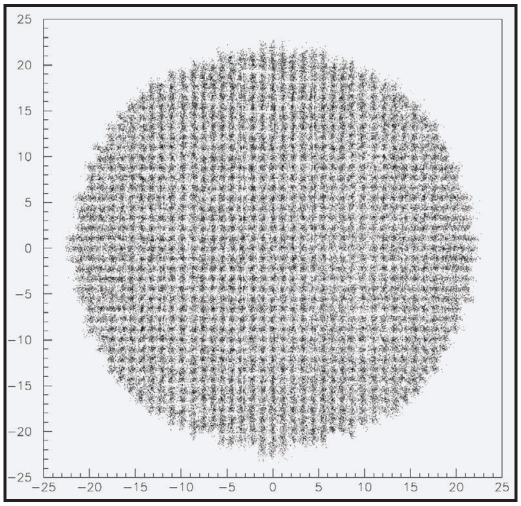

Fig.6. Planar image of a 4mm thick pixelated CsI(Tl) crystal after irradiation with a ^{60}Co point source. The position was reconstructed using the inverse method and most spatial distortions were removed after applying the position correction method. Distances are measured in mm.

B. Linearity Measurements

The deviation from linearity from both the planar images shown in Fig.5 was also estimated. The coordinates of each pixel along the central X and Y axes were extracted and directly compared, as shown in Fig.7.

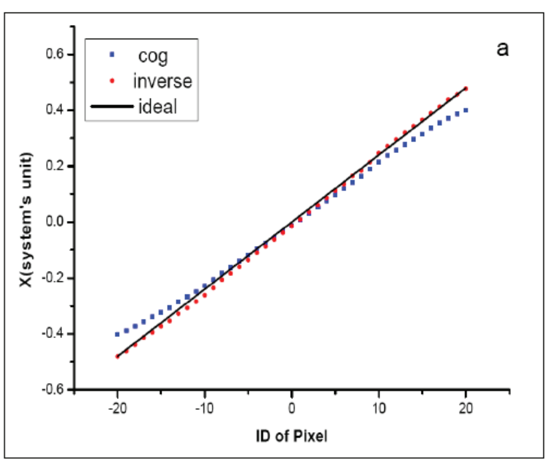

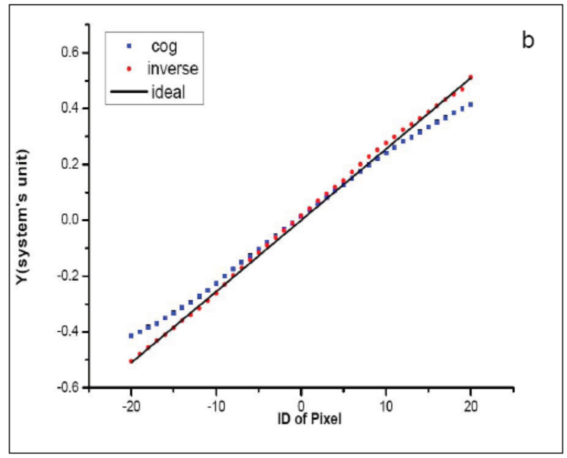

Fig.7. Position linearity graphs of the reconstructed coordinates for pixels along the central X (graph a) and Y (graph b) axis of images reconstructed with the extended model presented here (Fig.5). The blue points are the coordinates using the resistive chain algorithm and the red points using the inverse method. Black colored is the ideal line.

It is clear from Fig.7 that the reconstructed position based on the resistive chain algorithm deviates strongly from linearity. The deviation is greater as the distance from the center of the FOV is increasing. However, using the inverse method the linearity has almost been restored at both X and Y axes.

V. Discussion

The extended inverse method described in this work has been successfully applied to experimental data. The produced planar images have a better quality than the corresponding by the use of traditional resistive chain algorithm. The position linearity of the system is drastically improved and is almost restored. The extended inverse method combined with the position correction method based on a lookup table results to elimination of most of the spatial distortions. All these advantages make the inversion method presented in this work a very promising reconstruction technique for γ-Camera systems based on PSPMTs with a RCR.

References

[1] R. Pani *et al.*, "A novel compact gamma camera based on flat panel PMT", *Nucl. Instrum. and Methods A*, **513**, pp. 36-41, 2003.

[2] F. Sanchez *et al.*, "Performance tests of two portable mini gamma cameras for medical applications ", *Med. Phys.*, **33**, pp. 4210-4220, 2006.

[3] C. Trotta, R. Massari, N. Palermo, F. Scopinaro, A. Soluri, "New high spatial resolution portable camera in medical imaging", *Nucl. Instrum.and Methods A*, **577**, pp. 604-610, 2007.

[4] M. Mikeli *et al.*, "A New Position Reconstruction Method for Position Sensitive Photomultipliers", *2008 IEEE Nuclear Science Symposium Conference Record*, pp. 4736-4741.

[5] D. Thanasas *et al.*, "Correcting Spatial Distortion and non-Uniformity in Planar Images from γ-Camera Systems", *2008 IEEE Nuclear Science Symposium Conference Record*, pp. 3711-3714.